

## X-Ray Study on the Lattice Strains of Ferroelectric Iron Iodine Boracite $\text{Fe}_3\text{B}_7\text{O}_{13}\text{I}$

JINZO KOBAYASHI AND ISAO MIZUTANI

*Department of Applied Physics, Waseda University, Shinjuku-ku, Tokyo, Japan*

AND

HANS SCHMID AND HERBERT SCHACHNER

*Battelle Memorial Institute, Carouge, Geneva, Switzerland*

(Received 20 May 1969)

The accurate lattice parameters and the extremely small lattice strains of iron iodine boracite,  $\text{Fe}_3\text{B}_7\text{O}_{13}\text{I}$ , have been successfully measured over the paraelectric and the ferroelectric regions by using special x-ray diffraction methods. The spontaneous strains in the ferroelectric state could be separated into two parts, a linear strain (pure shear) and quadratic ones (electrostrictions). It is a conspicuous feature of the electromechanical properties of  $\text{Fe}_3\text{B}_7\text{O}_{13}\text{I}$  that the electrostrictions prevail over the linear strain induced through a torsional piezoelectric constant  $b_{36}$  of the paraelectric phase. The electrostrictive constants are approximately two orders of magnitude larger than those of  $\text{KH}_2\text{PO}_4$ . Another phase transformation at a lower temperature was disclosed by the present diffractometry. At this temperature a special rhombohedral lattice is formed, and the piezoelectric constant  $b_{36}$  vanishes.

### I. INTRODUCTION

IRON iodine boracite  $\text{Fe}_3\text{B}_7\text{O}_{13}\text{I}$ , one of the synthetic boracite crystals, undergoes a phase transformation from a high-temperature form  $T_d$ <sup>5</sup> to a low-temperature form  $C_{2v}$ <sup>5</sup> at 70°C.<sup>1</sup> We (J. K., H. S., and Ascher) have recently<sup>2</sup> proved the low-temperature form to be ferroelectric through optical observation of domain reversal under externally applied electric fields. According to our preliminary x-ray study, the lattice strains accompanied by the onset of ferroelectricity of the crystal were found to be too small to be detected by the usual x-ray diffractometry. On the other hand, it had already been reported by Ito *et al.*<sup>3</sup> that the same was the case for the mineral boracite  $\text{Mg}_3\text{B}_7\text{O}_{13}\text{Cl}$ . They reported that the conversion of the high- and the low-temperature forms was accompanied by no observable effect on the lattice dimensions and that x-ray powder photographs of both phases were practically identical.

Since the knowledge of the spontaneous lattice strains in the ferroelectric state must be of fundamental importance for the understanding of the mechanism of ferroelectricity of the boracite family, it seems urgent to determine the accurate lattice parameters and the lattice strains by any experimental means. We have undertaken a study of minute lattice strains in various ferroelectric boracites by using sensitive x-ray diffraction methods. This paper is concerned with  $\text{Fe}_3\text{B}_7\text{O}_{13}\text{I}$  as the first problem of this project.

### II. X-RAY DIFFRACTOMETRY

For the present measurements of the lattice parameters and the lattice strains, two x-ray diffraction methods have been used complementarily: a two-

dimensional reciprocal-lattice method and an x-ray strainmeter method, both developed by Kobayashi *et al.* The former<sup>4</sup> is laborious but indispensable for very accurate measurements of the absolute parameters; the latter<sup>5</sup> is promising for the detection of minute splittings of very close reflections and, accordingly, for accurate measurements of the lattice strains.

The orthorhombic  $C_{2v}$  phase of this crystal is based upon a slightly strained lattice of the cubic  $T_d$  phase, as a result of electromechanical coupling due to the spontaneous polarization; the pure shear  $x_{12}$ <sup>0</sup> occurs in a plane perpendicular to the ferroelectric axis, and in addition, the ferroelectric axis is strained by an electrostrictive effect. So it is convenient<sup>3,6</sup> to describe the lattice of  $\text{Fe}_3\text{B}_7\text{O}_{13}\text{I}$  in terms of the orthorhombic ( $A, B, C$ ) axes which are related to the cubic ( $a, b, c$ ) axes by a transformation matrix

$$\begin{pmatrix} \frac{1}{2} & \frac{1}{2} & 0 \\ -\frac{1}{2} & \frac{1}{2} & 0 \\ 0 & 0 & 1 \end{pmatrix},$$

as schematically depicted in Fig. 1. In what follows, the description will be given with reference to the ( $A, B, C$ ) axes, unless otherwise mentioned.

We prepared a small (100) plate specimen, 0.396 mm wide and 0.211 mm thick, as illustrated in Fig. 2. The narrow (001) planes were provided with electrodes of evaporated gold, and connected to a voltage source through a fine copper needle attached at one plane and a soft aluminum foil at the other. Upon application of a sufficiently high voltage of the proper polarity, the specimen changed its crystal orientation as shown in Fig. 2. Therefore, it was possible to get ( $h00$ ), ( $0k0$ ), and

<sup>4</sup> J. Kobayashi, N. Yamada, and T. Nakamura, Phys. Rev. Letters **11**, 410 (1963).

<sup>1</sup> H. Schmid, J. Phys. Chem. Solids **26**, 973 (1965).

<sup>2</sup> J. Kobayashi, H. Schmid, and E. Ascher, Phys. Status Solidi **26**, 277 (1968).

<sup>3</sup> T. Ito, N. Morimoto, and R. Sadanaga, Acta Cryst. **4**, 310 (1951).

<sup>5</sup> J. Kobayashi, N. Yamada, and T. Azumi, Rev. Sci. Instr. **39**, 1647 (1968).

<sup>6</sup> F. Jona and G. Shirane, *Ferroelectric Crystals* (Pergamon, New York, 1962), p. 70.

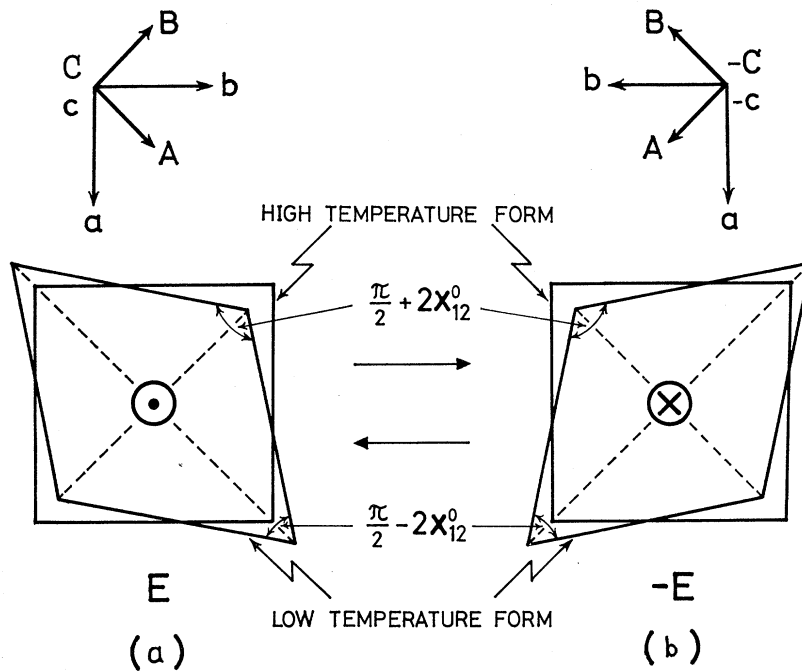


FIG. 1. Crystal lattices of high-temperature ( $T_d$ ) and low-temperature ( $C_{2v}$ ) forms of  $\text{Fe}_3\text{B}_7\text{O}_{13}\text{I}$  (distortion exaggerated) projected on (001). (a) and (b) differentiate the lattices under the applied electric fields  $E$  of opposite senses. The arrows between them indicate the reversal of the crystal orientations due to the fields, and the bold arrows perpendicular to the plane of the paper indicate the senses of the spontaneous polarization.

(00 $l$ ) reflections from the same crystal mounting. In order to confirm the specimen to be single domain during the measurements, and, further, to establish the relation between the crystallographic axes and the refractive indices of the respective directions, the specimen on the

goniometer head was inspected by placing it diagonally with respect to the crossed polaroids mounted on the x-ray diffractometer. Thus the optical orientation of the specimen in the measuring processes was easily known by observing its interference colors, since the relation

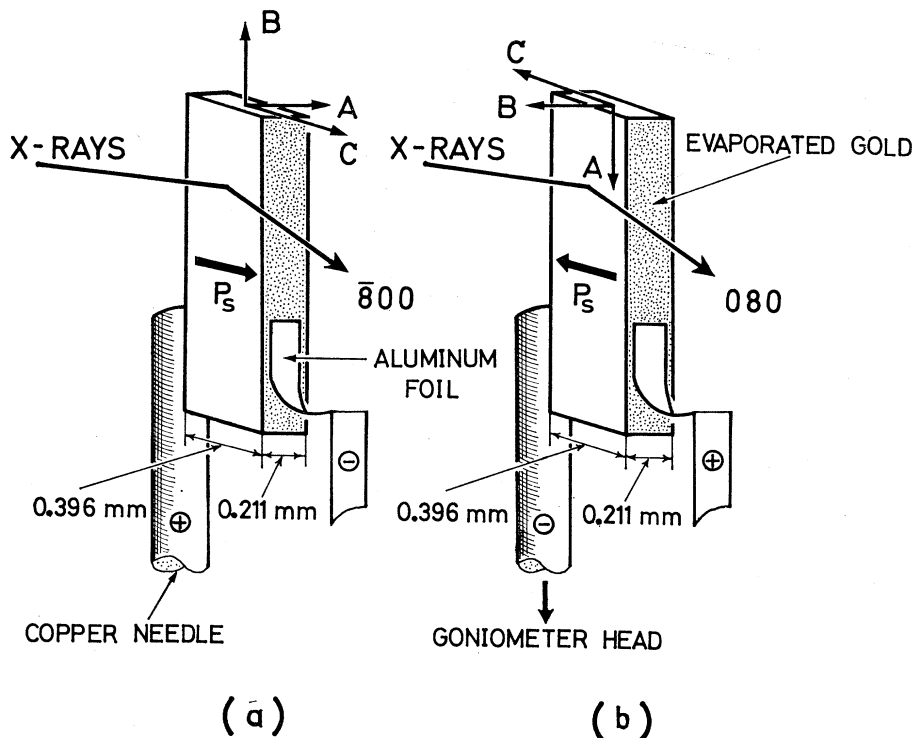


FIG. 2. Sketch of the x-ray specimen of  $\text{Fe}_3\text{B}_7\text{O}_{13}\text{I}$  on the goniometer head of the spectrometer. The orientations, (a) and (b), correspond to those in Fig. 1.

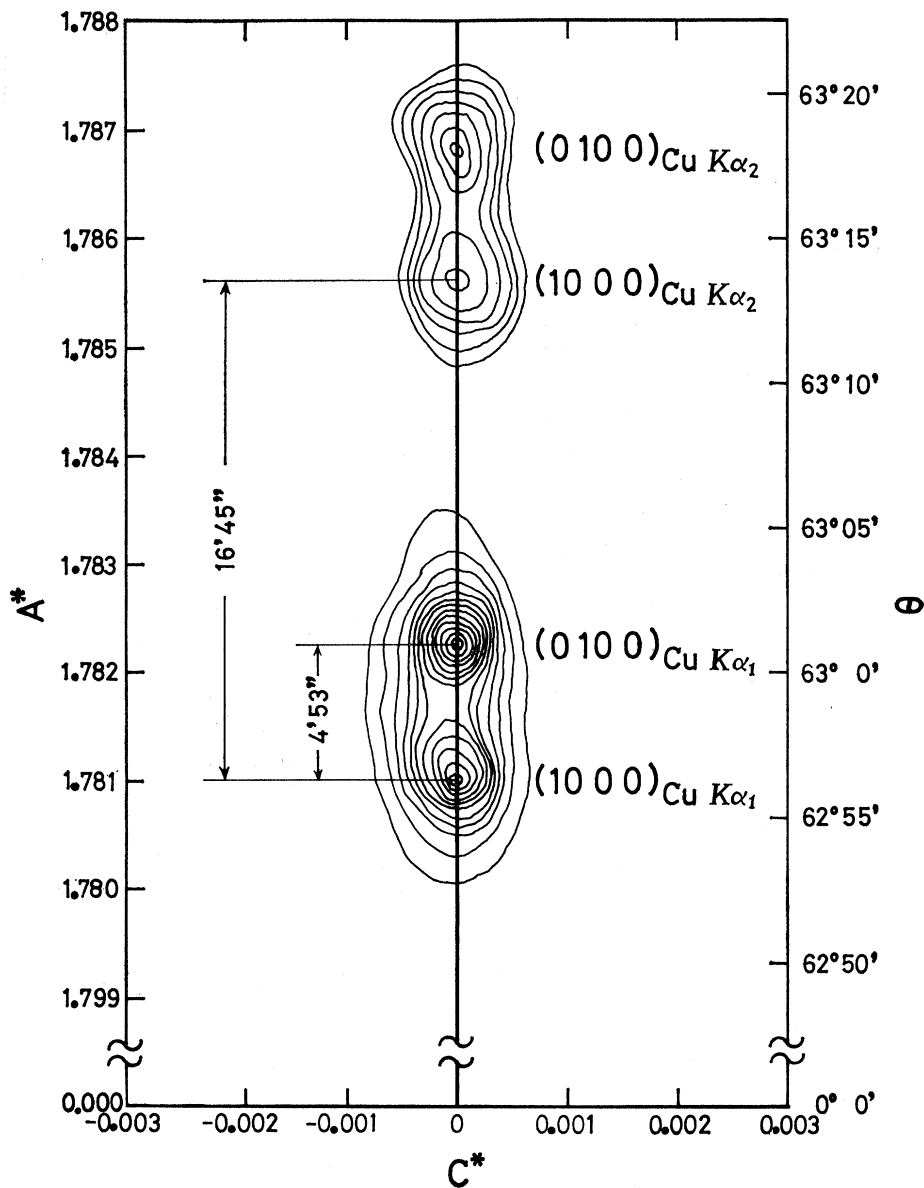


FIG. 3. Two-dimensional intensity distribution of (10 0 0) and (0 10 0) reflections ( $T=25.5^{\circ}\text{C}$ ) from the specimen of  $\text{Fe}_2\text{B}_7\text{O}_{13}\text{I}$  containing two  $180^{\circ}$  domains. The abscissa stands for the  $C^*$  axis and the ordinate for the  $A^*$  axis expressed in the unit of  $d^*=2 \sin\theta$ . The data were obtained by rotating the crystal and a detector separately in the same  $A^*-C^*$  plane. At every small successive rotation  $\Delta\theta$  of the crystal, the intensities of diffraction taking place in a variety of directions, corresponding to the intersection of the sphere of reflection with the intensity distribution, were scanned by a scintillation counter as a function of  $2\theta$ .

between the interference colors and three mutually perpendicular directions has already been studied.<sup>2</sup> The measurements were carried out from  $118$  to  $-90^{\circ}\text{C}$ , the temperatures of the specimen being kept constant within the limit of  $\pm 0.1^{\circ}\text{C}$  during the measurements. The x-ray radiation used was unfiltered  $\text{Cu } K\alpha$ .

We first measured the absolute lattice parameters accurately at various temperatures by using the two-dimensional reciprocal-lattice method. The principle and the technical performance have already been described earlier.<sup>4</sup> The important feature of a precise reading of the reflecting angle  $\theta$  by this method is to map out a complete two-dimensional intensity distribution around the reciprocal-lattice point in a proper reciprocal-lattice plane by using the following data;

at every small successive rotation  $\Delta\theta$  of the crystal ( $0.01^{\circ}$  in the present case) in the vicinity of maximum-reflection position, the diffraction intensities are recorded by a detector as a function of  $2\theta$ . As an example of the present experiments, Fig. 3 illustrates the intensity distribution of (10 0 0) and (0 10 0) reflections ( $T=25.5^{\circ}\text{C}$ ) from the crystal which was found by optical checking to consist of two distinct  $180^{\circ}$  domains corresponding, respectively, to Figs. 2(a) and 2(b). Thus, the very close reflections at issue are well resolved.

Such measurements are extremely precise but not sufficiently accurate without elimination of systematic errors. The prominent systematic errors introduced here would be the absorption of x rays by the specimen and

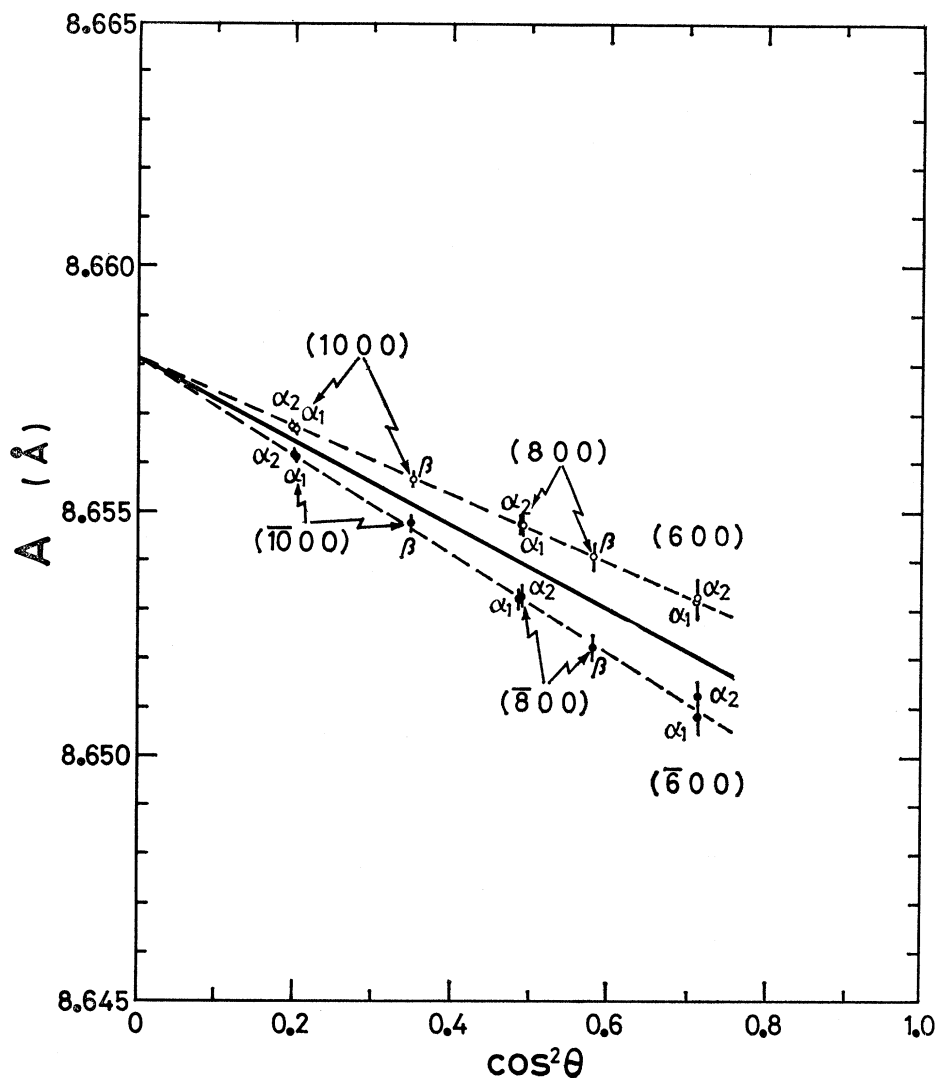


FIG. 4. Extrapolation procedure for getting the  $A$  parameter at  $19.5^\circ\text{C}$  for  $\text{Cu } K\alpha$  and  $\beta$ . There are two branches of dashed lines for  $(h00)$  and  $(\bar{h}00)$  series. A solid straight line between them represents the extrapolation by the  $A$  values, free from eccentricity error.

the eccentricity of the specimen-position in the diffractometer. The absorption error was especially serious in the present experiments because the wavelengths of  $\text{Cu } K\alpha$  are close to the absorption edge of iron. In the present case,  $\mu R$  was approximately estimated as 10.6, where  $\mu$  is the linear absorption coefficient and  $R$  is the mean radius of the cross section of the specimen. In order to remove these errors, we used the extrapolation method<sup>7</sup> at several temperatures. At a fixed temperature, two series of measurements were carried out. In order to get the  $A$  parameter, for instance, several  $(h00)$  reflections and their rear  $(\bar{h}00)$  reflections, which were brought about by rotating the specimen by  $180^\circ$  around the  $B$  axis, were drawn on an  $(h0l)$  reciprocal-lattice plane. An extrapolation procedure for the  $A$  parameter at  $19.5^\circ\text{C}$  is indicated in Fig. 4, where the  $A$  values derived from all the reciprocal-lattice maps

are plotted against  $\cos^2\theta$ . The extrapolation consists of two branches of dashed straight lines corresponding to  $(h00)$  and  $(\bar{h}00)$  series. The discrepancy between the two branches measures the eccentricity of the specimen position, while the mean slope of the lines (depicted by a solid line in the figure) depends solely on the absorption. The convergence of the extrapolation of the two branches at  $\theta=90^\circ$  was excellent at every measured temperature. This fact means that the extrapolation method for attaining high accuracy is correct and our readings of the reflection positions by the reciprocal-lattice method were precise. All the parameters thus obtained were corrected for refraction of x rays to the crystal. They were divided by the calculated refractive index for  $\text{Cu } K\alpha$ , 0.999987. After such treatments we attained a precision and accuracy of one part in 227 000 for the present measurements of the lattice parameters.

On the other hand, the temperature change of the small strains could be unequivocally demonstrated and

<sup>7</sup> A. J. Bradley and A. H. Jay, Proc. Phys. Soc. (London) 44, 563 (1932).

determined by the photographic films taken by the x-ray strainmeter, which has recently been developed.<sup>5</sup> Figure 5 shows x-ray photographs of  $\text{Fe}_3\text{B}_7\text{O}_{13}\text{I}$  taken at successive temperatures over both cubic and orthorhombic forms, where two reflections ( $\bar{8}00$ ) and (080) are taken in the same row by a double exposure. The splittings of these spectra are satisfactorily large. Thus, the lattice strains could be obtained accurately from these films.

### III. EXPERIMENTAL RESULTS

The lattice parameters and the thermal-expansion coefficients along the  $A$ ,  $B$ , and  $C$  axes at several temperatures are given in Table I. Temperature dependence of the lattice parameters and the lattice volume are expressed in Fig. 6. With decreasing temperature, the cubic cell edge (represented by both  $c$  and  $c/\sqrt{2}$  in the figure) decreases linearly. At the ferroelectric Curie point  $T_c$  of  $72^\circ\text{C}$ , not only the ferroelectric  $C$  axis, but also the  $A$  and  $B$  axes abruptly elongate. In the ferroelectric state, the  $C$  and  $A$  axes decrease slightly, while the  $B$  axis increases almost linearly and finally coalesces with the  $A$  axis at  $-70^\circ\text{C}$ . This temperature coincides with the lower transition point from  $C_{2v}$  to trigonal  $C_{3v}$  phase, which has already been evidenced by both Mössbauer and optical studies.<sup>8</sup> With increasing temperature, the lower transition point shifts to  $-55^\circ\text{C}$  as a result of large thermal hysteresis, while the Curie point also shifts slightly. It may be noted that at the lower transition point the length of the  $C$  axis becomes exactly  $\sqrt{2}$  times as large as those of the  $A$  and  $B$  axes, that is to say, the three cubic ( $a, b, c$ ) axes become equal in length. It follows that at this temperature a special rhombohedral lattice is formed, in which the lengths of the three axes happen to be equal, and the three axial angles are  $90^\circ$ . Below the transition point, the axial angles remain equal to each other but differ from  $90^\circ$ . The detailed account of the trigonal phase will be reported in a subsequent paper.

From the optical observations,<sup>9</sup> it has become clear that the refractive indices of the  $C_{2v}$  phase with regards

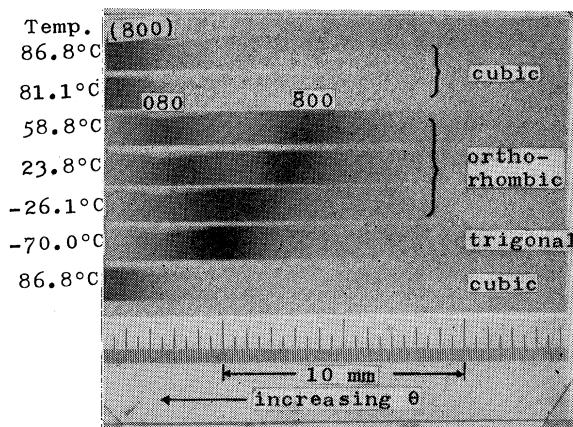


FIG. 5. X-ray photographs of ( $\bar{8}00$ ) and (080) reflections of  $\text{Fe}_3\text{B}_7\text{O}_{13}\text{I}$  taken by the x-ray strainmeter at successive temperatures, showing that two phase transformations occur. Each photograph is the result of a double exposure, one for each orientation shown in Fig. 2. During the exposures the specimen was allowed to oscillate within an angle of  $40'$  containing the maximum-reflection position.

to the light vibrating along the  $A$ ,  $B$ , and  $C$  axes are  $n_\beta$ ,  $n_\gamma$ , and  $n_\alpha$ , respectively.

The spontaneous strains  $x_1$ ,  $x_2$ , and  $x_3$  along the  $A$ ,  $B$ , and  $C$  axes, which occur by virtue of the spontaneous polarization, are calculated by referring to the extrapolated  $A$  and  $C$  axes of the cubic phase into the ferroelectric region. They are shown in Fig. 7 as a function of temperature.

### IV. DISCUSSION

The paraelectric phase of  $\text{Fe}_3\text{B}_7\text{O}_{13}\text{I}$  ( $T_d$  class) has the torsional piezoelectric coefficients  $b_{14}^p$ ,  $b_{25}^p$ , and  $b_{36}^p$  defined, referring to the cubic lattice directions. They are all identical in sign and in magnitude. Therefore, under the existence of an electric polarization  $P_3$ , a pure shear  $x_{12}^0 = \frac{1}{2}b_{36}^p P_3$  occurs.<sup>10</sup> The ferroelectric modification ( $C_{2v}$  class) can be then conceived as a state where the symmetry is lowered, owing to the occurrence of the spontaneous polarization  $P_s$  along the  $C$  direction. In this sense, the present data will be discussed in the light of phenomenological theory.

TABLE I. Lattice parameters and thermal-expansion coefficients along the orthorhombic  $A$ ,  $B$ , and  $C$  axes of  $\text{Fe}_3\text{B}_7\text{O}_{13}\text{I}$ .

Temperature ( $^\circ\text{C}$ )	Lattice parameters ( $\text{\AA}$ )			Thermal-expansion coefficients		
	$A$	$B$	$C$	$\alpha_A$ ( $10^{-6}$ )	$\alpha_B$ ( $10^{-6}$ )	$\alpha_C$ ( $10^{-6}$ )
110.3	$8.65012 \pm 0.000039$	$8.65012 \pm 0.000039$	$12.23312 \pm 0.000055$	5.7	5.7	5.7
80.1	$8.64860 \pm 0.000037$	$8.64860 \pm 0.000037$	$12.23096 \pm 0.000052$	5.7	5.7	5.7
70.2	$8.65951 \pm 0.000037$	$8.65152 \pm 0.000037$	$12.24055 \pm 0.000052$	0.0	0.0	0.0
29.8	$8.65879 \pm 0.000035$	$8.65191 \pm 0.000035$	$12.24034 \pm 0.000049$	5.0	-1.9	3.4
-10.0	$8.65693 \pm 0.000037$	$8.65259 \pm 0.000037$	$12.23915 \pm 0.000052$	5.3	-2.2	2.6
-49.6	$8.65511 \pm 0.000039$	$8.65331 \pm 0.000039$	$12.23787 \pm 0.000055$	5.3	-2.2	2.6

<sup>8</sup> H. Schmid and J. M. Trooster, *Solid State Commun.* **5**, 31 (1967).

<sup>9</sup> J. Kobayashi and I. Mizutani (unpublished).

<sup>10</sup> Reference 6, p. 18.

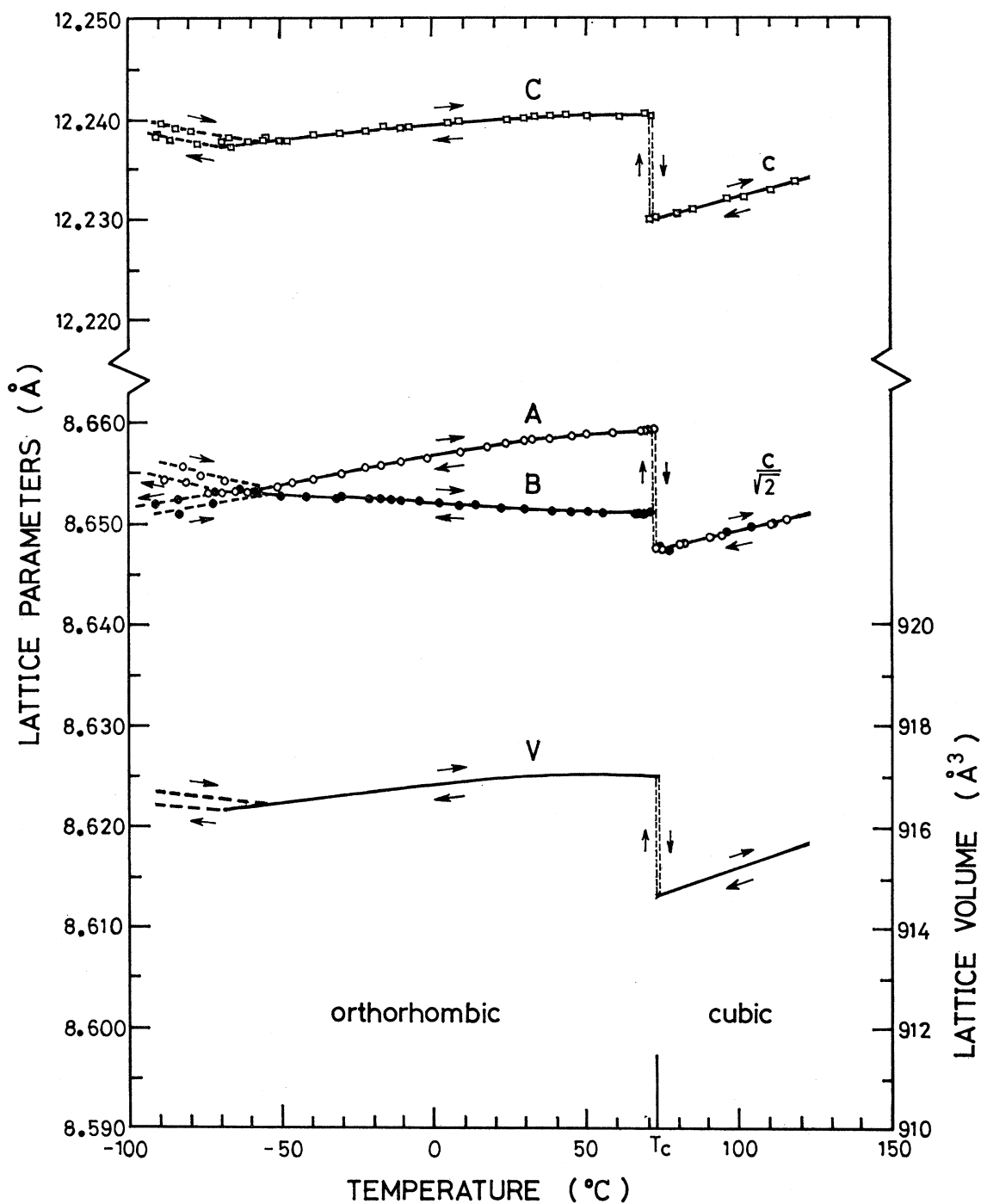


Fig. 6. Temperature dependence of the  $A$ ,  $B$ , and  $C$  lattice parameters, and the lattice volume  $V$  of  $\text{Fe}_3\text{B}_7\text{O}_{13}\text{I}$ .

The piezoelectric coefficients of  $T_d$  phase, when referred to the axes parallel to the  $(A, B, C)$  axes, are expressed in terms of  $b_{36}^p$  as follows<sup>11</sup>:

$$b_{15} = -b_{24} = 2b_{31} = -2b_{32} = b_{36}^p.$$

When the polarization  $P_s$  occurs along the  $C$  axis, the

<sup>11</sup> Reference 6, p. 76.

strains  $x_1$ ,  $x_2$ , and  $x_3$  will be developed along the  $A$ ,  $B$ , and  $C$  axes as

$$\begin{aligned} x_1 &= \frac{1}{2}b_{36}^p = x_{12}^0, \\ x_2 &= -\frac{1}{2}b_{36}^p P_s = -x_{12}^0, \\ x_3 &= 0. \end{aligned}$$

In the ferroelectric  $C_{2v}$  phase,  $b_{31}$  and  $b_{32}$  become un-

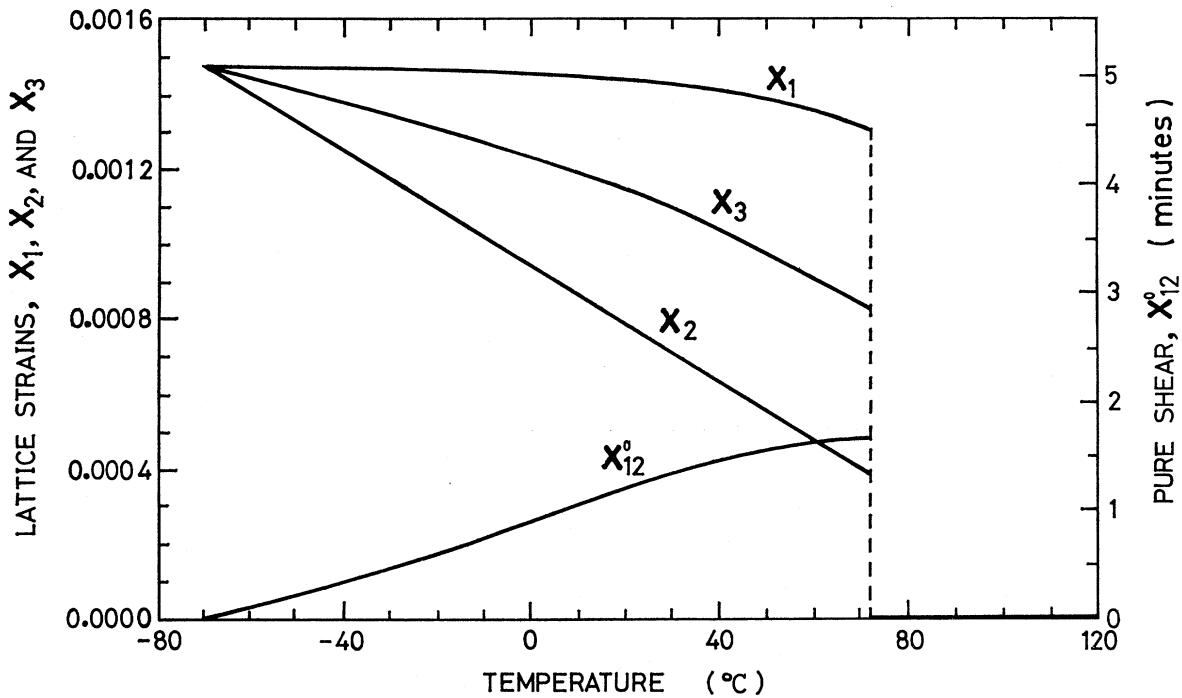


FIG. 7. Spontaneous lattice strains  $x_1$ ,  $x_2$ , and  $x_3$  along the  $A$ ,  $B$ , and  $C$  axes of the ferroelectric  $\text{Fe}_3\text{B}_7\text{O}_{13}\text{I}$  as a function of temperature. The pure shear  $x_{12}^0$  in a plane perpendicular to the ferroelectric axis is also indicated.

equal in magnitude and  $b_{33}$  becomes nonzero.<sup>11</sup> Since the origin of these changes is ascribed to the occurrence of  $P_s$ , they can be written as follows:

$$\begin{aligned} b_{31} &= \frac{1}{2}b_{36}P_s + Q_{31}P_s, \\ b_{32} &= -\frac{1}{2}b_{36}P_s + Q_{32}P_s, \\ b_{33} &= Q_{33}P_s, \end{aligned}$$

where  $Q_{31}$ ,  $Q_{32}$ , and  $Q_{33}$  are electrostrictive constants in the  $C_{2v}$  phase. Since it has been proved experimentally in all the ferroelectrics ever studied that such higher-rank tensors as the electrostrictive constants are almost temperature-independent over ferroelectric phase transitions, we assume as a good approximation that both  $Q_{31}$  and  $Q_{32}$  are equal to  $Q_{31}^0$  of the paraelectric  $T_d$  phase and that  $Q_{33}$  also equals  $Q_{33}^0$  of the same phase. Then the strains under the spontaneous polarization  $P_s$  can be expressed as

$$\begin{aligned} x_1 &= \frac{1}{2}b_{36}P_s + Q_{31}^0P_s^2 = x_{12}^0 + Q_{31}^0P_s^2, \\ x_2 &= -\frac{1}{2}b_{36}P_s + Q_{31}^0P_s^2 = -x_{12}^0 + Q_{31}^0P_s^2, \\ x_3 &= Q_{33}^0P_s^2. \end{aligned}$$

From the above equations, we get the following formulas:

$$\begin{aligned} x_{12}^0 &= \frac{1}{2}b_{36}P_s = \frac{1}{2}(x_1 - x_2), \\ Q_{31}^0 &= \frac{1}{2}(x_1 + x_2), \\ Q_{33}^0P_s^2 &= x_3. \end{aligned}$$

Thus, it is possible to obtain separately the linear piezoelectric strain  $\frac{1}{2}b_{36}P_s$ , which is the pure shear  $x_{12}^0$  of the cubic lattice, and the quadratic strains  $Q_{31}^0P_s^2$  and  $Q_{33}^0P_s^2$ . In Fig. 8 these quantities are expressed with regards to temperature.

The pure shear is developed suddenly at the Curie point, decreases with decreasing temperature, and finally diminishes to zero at the lower transition point. It must be noted that the magnitude of the electrostriction  $Q_{31}^0P_s^2$  along the  $A$  and  $B$  axes is more than twice as large as the linear strain. This is one of the conspicuous features of the electromechanical properties of  $\text{Fe}_3\text{B}_7\text{O}_{13}\text{I}$ . It is interesting to compare the electromechanical properties with those of  $\text{KH}_2\text{PO}_4$ , which has been supposed to reveal a typical "shear transformation" at the onset of ferroelectricity. The shear of  $\text{Fe}_3\text{B}_7\text{O}_{13}\text{I}$  is extremely small, i.e., a maximum value being  $1'38''$  at  $T_c$ , whereas in  $\text{KH}_2\text{PO}_4$  it is  $13'30''$  at  $20^\circ\text{C}$  below  $T_c$ .<sup>12</sup> von Arx and Bantle<sup>13</sup> discovered that in  $\text{KH}_2\text{PO}_4$  the spontaneous strains  $x_1$  and  $x_2$  perpendicular to the ferroelectric axis are the sum of the linear and the electrostrictive terms, as is the case for  $\text{Fe}_3\text{B}_7\text{O}_{13}\text{I}$ , and the latter is an order of magnitude smaller than the former. Therefore, it is certain that the electrostrictive nature plays an imperative role in the transition mechanism of this boracite crystal.

<sup>12</sup> M. de Quervain, *Helv. Phys. Acta* **17**, 509 (1944).

<sup>13</sup> A. von Arx and W. Bantle, *Helv. Phys. Acta* **17**, 298 (1944).

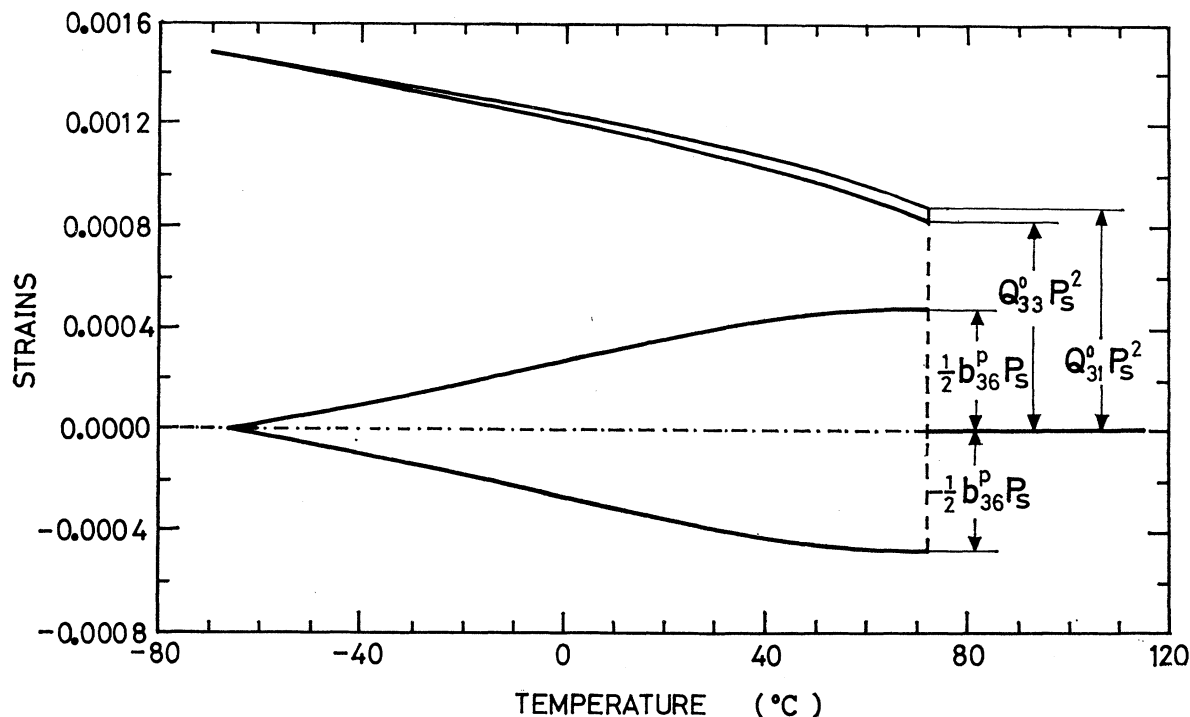


FIG. 8. Temperature dependence of the linear piezoelectric strain  $\frac{1}{2}b_{36}^p P_s$  (pure shear  $x_{12}^0$ ), and the quadratic strains  $Q_{31}^0 P_s^2$  and  $Q_{33}^0 P_s^2$  in the ferroelectric state of  $\text{Fe}_3\text{B}_7\text{O}_{13}\text{I}$ .

$Q_{31}^0$  and  $Q_{33}^0$  are nearly equal in magnitude in the entire ferroelectric region and coincide perfectly with each other at the lower transition temperature. Since these quantities are supposed to be almost temperature independent from the paraelectric phase, the behavior of  $Q_{31}^0 P_s^2$  and  $Q_{33}^0 P_s^2$  shown in Fig. 8 should reflect the temperature variation of  $P_s^2$ . This supposition has been proved to be correct by our recent measurements of the spontaneous polarization.<sup>14</sup> Then it follows that  $b_{36}^p$  begins to decrease from the Curie point monotonically and vanishes at the lower transition point in the same way as  $x_{12}^0$ . The calculated values of electromechanical

constants of  $\text{Fe}_3\text{B}_7\text{O}_{13}\text{I}$  are given as follows:

$$Q_{31}^0 \simeq Q_{33}^0 = 1.1 \pm 0.5 \times 10^{-10} \text{ esu}$$

$$(Q_{31}^0 = 3.84 \times 10^{-12} \text{ esu}, \quad Q_{33}^0 = 2.9 \times 10^{-12} \text{ esu}^{15}),$$

$$b_{36}^p = 1.8 \pm 0.5 \times 10^{-7} \text{ esu} \quad (21^\circ\text{C}) \quad (5.0 \times 10^{-7} \text{ esu}^{15}),$$

where the corresponding values of  $\text{KH}_2\text{PO}_4$  are shown in parentheses for the sake of comparison. Thus, it is seen that the electrostrictive constants in  $\text{Fe}_3\text{B}_7\text{O}_{13}\text{I}$  are two orders of magnitude larger than those of  $\text{KH}_2\text{PO}_4$ . We suggest that in the course of elucidation of the ferroelectric behavior of  $\text{Fe}_3\text{B}_7\text{O}_{13}\text{I}$ , the peculiar electromechanical property disclosed here must always be taken into account.

<sup>14</sup> J. Kobayashi and I. Mizutani (unpublished).

<sup>15</sup> Reference 6, p. 72.



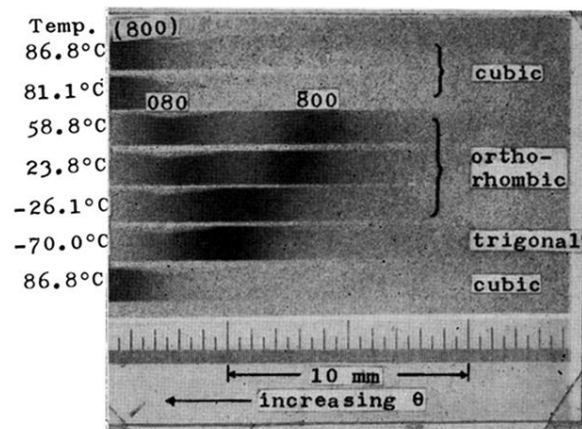


FIG. 5. X-ray photographs of  $(\bar{8}00)$  and  $(080)$  reflections of  $\text{Fe}_3\text{B}_7\text{O}_{13}\text{I}$  taken by the x-ray strainmeter at successive temperatures, showing that two phase transformations occur. Each photograph is the result of a double exposure, one for each orientation shown in Fig. 2. During the exposures the specimen was allowed to oscillate within an angle of  $40'$  containing the maximum-reflection position.